UNIVERSITY OF WISCONSIN-LA CROSSE

Graduate Studies

EVALUATION OF COPPER ALLOY SURFACES FOR INACTIVATION OF TULANE VIRUS, A HUMAN NOROVIRUS SURROGATE, AND HUMAN NOROVIRUSES

A Manuscript Style Thesis Submitted in Partial Fulfillment of the Requirements for the Degree of Master of Science

Jordan Recker

College of Science and Health

Microbiology

May, 2018

EVALUATION OF COPPER ALLOY SURFACES FOR INACTIVATION OF TULANE VIRUS, A HUMAN NOROVIRUS SURROGATE, AND HUMAN NOROVIRUSES

By Jordan Recker

We recommend acceptance of this thesis in partial fulfillment of the candidate's requirements for the degree of Masters of Science in Microbiology

The candidate has completed the oral defense of the thesis.

4-27-2018
Xinhui Li, Ph.D. — Date
Thesis Committee Chairperson

4-27-18
Michael Hoffman, Ph.D. — Date
Thesis Committee Member

4/27/18
Marc Rott, Ph.D. — Date
Thesis Committee Member

4/27/18
Peter Wilker, Ph.D. — Date
Thesis Committee Member

Thesis accepted

6-1-18
Meredith Thomsen, Ph.D. — Date
Graduate Studies Director

ABSTRACT

Recker, J.D. Evaluation of copper alloy surfaces for inactivation of Tulane virus, a human norovirus surrogate, and human noroviruses. MS in Microbiology, May 2018, 62pp. (X. Li)

This study evaluated the efficacy of copper alloy surfaces for inactivation of Tulane virus, a human norovirus surrogate, using plaque assay and porcine gastric mucin-conjugated magnetic beads (PGM-MB) binding assay followed by quantitative reverse transcription-PCR (PGM-MB/PCR assay). Additionally, the sensitivities of human norovirus GII.4 Sydney and GI.3B Potsdam strains to copper alloy surfaces were assessed using PGM-MB/PCR assay. Time-dependent inactivation of viruses on copper alloy coupons revealed that, for Tulane virus, 15 min of copper alloy surface treatments achieved more than 4-log reductions, as assessed by plaque assay, while up to 20 min of copper alloy surface treatments only achieved ~2-log reductions, as assessed by PGM-MB/PCR assay. As assessed by PGM-MB/PCR assay, 10 min of copper surface treatments achieved reductions of 3 and 4 log units for human norovirus GII.4 Sydney and GI.3B Potsdam, respectively. Results from this study suggest that even though PGM-MB/PCR assay underestimated the efficacy of copper alloy surface inactivation of Tulane virus, copper alloys could effectively inactivate Tulane virus and human noroviruses. Therefore, copper alloys can be used as a preventive measure to prevent human norovirus infection and an effective surface treatment for human noroviruses.

Acknowledgements

I would like to thank my thesis advisor, Dr. Xinhui Li for his guidance and support during my graduate studies. I would also like to thank me three other committee members, Dr. Michael Hoffman, Dr. Marc Rott, and Dr. Peter Wilker for their encouragement and advice. Along with my committee members, I would also like to graciously say thank you to Dr. Bernadette Taylor for allowing me to use her lab space and biosafety cabinet for my research. I am also appreciative of the UW-La Crosse Department of Microbiology for help with advice and instruction. I am grateful for the generous help from the Statistical Consulting Center, specifically Dr. Abdulaziz Elfessi, for guidance during the statistical analysis of my thesis.

I sincerely appreciate Dr. Li's UW-La Crosse start-up funds, UW-La Crosse Graduate Student Research, Service, and Educational Leadership Grant, Graduate Professional Travel Grant, and the Microbiology Graduate Summer Research Fellowship for funding and stipends.

Lastly, I would like to thank all of my friends, classmates, fellow graduate/teaching assistants, and family members for their support and encouragement throughout my graduate experience. I truly would not be the person I am today without the impact everyone mentioned has made on me.

TABLE OF CONTENTS

PAGE

LIST OF FIGURES

FIGURE PAGE

LIST OF TABLES

TABLE PAGE

INTRODUCTION

Foodborne Viruses

Even though bacteria have been associated with foodborne outbreaks and illnesses, it is acknowledged that viruses are the major cause of foodborne illnesses (https://www.cdc.gov/foodsafety/foodborne-germs.html) (1, 2). Foodborne viruses are mostly transmitted through the fecal-oral route via contaminated food and water or person-to-person contact, but some can also be transmitted via aerosols containing the viruses (3–5).

There are many types of viruses that cause foodborne illnesses, but these viruses can be broken down into three main groups based on the illnesses they cause (6):

1. Enterically transmitted hepatitis viruses, such as hepatitis A and hepatitis E.
2. Viruses that replicate in the human gut but disseminate to other parts of the body and cause illnesses, such as poliovirus.
3. Viruses causing gastroenteritis, such as rotavirus, sapovirus, and human noroviruses (HuNoVs).

Viruses are strict intracellular parasites and they cannot replicate in food or water, therefore, viruses that contaminate food and water cannot increase in number (6). Fruits, vegetables, and shellfish are common types of food products associated with foodborne viruses because they could be contaminated before harvest and only minimally processed before consumption. Besides contamination before harvest, infected workers or food

handlers are also common sources of foodborne viruses to the human population (1, 6, 7). Most foodborne viruses are non-enveloped, have a low infectious dose, and are shed in high numbers in stool or vomit (6). These characteristics contribute to the survivability of foodborne viruses in/on the food products and the successful transmission of the viruses.

According to the Centers for Disease Control and Prevention (CDC), there are 37.2 million foodborne illnesses each year in the United States and 59% of the infections are caused by foodborne viruses (8). Even though viruses cause a majority of foodborne illnesses, viral infections tend to be less severe, as viruses only account for 27% of hospitalizations and 12% of deaths due to foodborne illnesses (8). There are several foodborne viruses that commonly cause foodborne outbreaks and illnesses. Rotavirus has been a prominent foodborne virus that causes gastroenteritis in children, causing 70,000 hospitalizations per year among United States children (9, 10). Before the rotavirus vaccine, more than 80% of children were infected with rotavirus by the age of five (11). In 2006, two oral rotavirus vaccines were implemented and have drastically reduced the amount of gastroenteritis caused by rotavirus, with national declines of rotavirus ranging from 58%-90% (9, 10). Hepatitis A virus (HAV) and hepatitis E virus (HEV) are two other common foodborne viruses in circulation (1). There are approximately 1.4 million cases of HAV and 200 million asymptomatic carriers each year globally (1). HAV has been associated with outbreaks caused by contaminated seafood, vegetables, and berries (1). In 2013, a frozen berry mix was contaminated with HAV and at least 158 individuals in the United States were infected, resulting in 69 hospitalizations (1). In 2016, another multistate outbreak of hepatitis linked to HAV caused 143 cases and 56 hospitalizations due to contaminated frozen strawberries

(https://www.cdc.gov/hepatitis/outbreaks/2016/hav-strawberries.htm). Annually, HEV accounts for over 20 million global infections and are associated with contaminated water and consumption of undercooked meats and shellfish (1). Lastly, the most common foodborne illness is caused by HuNoVs, which was the main focus of this study and will be discussed more in the following section (12–14).

Human Noroviruses

Clinical Significance

HuNoVs are the leading cause of foodborne illness and are a worldwide public health concern (12, 13, 15). According to the CDC, there are approximately 21 million infections that cause between 50,000-71,000 hospitalizations and 570-800 deaths in the United States each year (16). HuNoVs cause gastroenteritis, with symptoms including nausea, vomiting, diarrhea, and low-grade fevers that can last up to 48 hours in immunocompetent individuals (16). Even though HuNoVs usually cause an acute gastroenteritis that will clear up within days of infection, different risk groups including young children, elderly individuals, transplant patients, and citizens of developing countries can have more severe and longer gastroenteritis symptoms (16). In developing countries, there are over one million hospitalizations and 200,000 deaths per year from the HuNoV (16, 17). Young children can develop more severe infections and can have symptoms lasting up to six weeks (16). Transplant patients and immunosuppressed individuals can also have prolonged symptoms that can last over two years (16).

Similar to many other foodborne viruses, spread of HuNoVs usually occurs via the fecal-oral route from contaminated food and water (12, 13, 15, 18). Seafood, produce,

and other raw foods have been associated with HuNoV outbreaks (12, 15). In addition, infections can also be caused by direct contact from another infected individual or ingestion of aerosolized particles (13, 18–20). High shedding of virus is a common characteristic of HuNoV cases, with 10^5-10^{11} particles per gram of feces. Since HuNoV has an infectious dose of only 18 virus particles, HuNoVs are highly contagious (20). These characteristics lead to HuNoV outbreaks in close-quarter environments such as cruise ships, schools, restaurants, and care facilities (13).

Currently, PCR-based assays are used to diagnose HuNoVs. However, if it is not possible to get lab-confirmed norovirus, the Kaplan criteria are used to determine a HuNoV outbreak. The Kaplan Criteria are: >50% of the infected individuals must have vomiting, a mean incubation period of 24-48 hours, a mean illness duration of 12-60 hours, and have no bacterial pathogens recovered from stool samples (18, 21).

HuNoVs are stable in varying environments, persisting in temperatures ranging from freezing to 63°C, and are resistant to many common disinfectants and alcohol-based hand sanitizers (20, 22). For example, Richards *et al*. demonstrated that HuNoV particles were stable and still infectious for at least 14 freeze/thaw cycles at -80°C (23). The researchers also showed that HuNoV particles survived long-term frozen storage (23). Liu *et al*. and Tung *et al.* tested the efficacy of ethanol based hand sanitizers and bleach on the inactivation of HuNoVs (24, 25). The researchers found that ethanol based hand sanitizers were not effective at inactivating HuNoV with 95% ethanol (24, 25). Studies also showed at least 1,000 ppm of bleach was needed to obtain significant inactivation of HuNoV (24, 25). A study has also showed infectious viral particles persisting on contaminated surfaces for weeks (26).

Human noroviruses cause a large global burden, causing around $4.2 billion in health system costs and $60.3 billion in societal costs, with loss of productivity serving as the largest percentage of the burden (27). Effective prevention and control methods are very difficult because of the complex transmission routes and high genetic variability of the virus (28). With this impact, HuNoVs are a high priority public health issue, and development of a HuNoV vaccine is desired. Bartsch *et al*. reported that a theoretical HuNoV vaccine with 75% efficacy for 48 months of protection and a cost of $50 could prevent up to 48,000 hospitalizations and save between $100 million and $2.1 billion in the United States each year (29). The lack of a vaccine is largely due to the difficulties in cultivating HuNoVs and a broad range of genetic diversity of HuNoVs. The diversity of circulating HuNoV strains is a result of mutations and recombination events between norovirus genotypes in co-infected individuals. The high diversity presents challenges in the development of vaccines (30). Currently, there are two vaccines that have reached the clinical trial stage and many other candidate vaccines are in pre-clinical stages of vaccine development (30). Therefore, until a vaccine is licensed for use, precautionary measures to prevent HuNoV infections by washing hands, environmental disinfection, and isolating infected individuals are the best defenses against infection (20).

HuNoV Classification

HuNoVs belong to the genus *Norovirus* of the family *Caliciviridae*, which is in the order *Picornavirales*. Within the *Caliciviridae* family, there are the *Lagovirus, Nebovirus, Vesivirus, Sapovirus*, *Norovirus*, and the novel *Recovirus* genera (31, 32). The genus *Sapovirus* includes sapovirus, another foodborne virus that also causes gastroenteritis in humans (1).

Norovirus is an extremely diverse genus that includes 5 different genogroups (16, 18, 33). Individual genogroups are designated by a capital "G" and a Roman numeral (Fig. 1). Within the 5 genogroups, GI, GII, and GIV affect humans, with GI and GII most frequently associated with outbreaks (4, 16, 34). Genogroups are further broken down into genotypes and are designated with an Arabic numeral (Fig. 1) (18). Genogroups GI and GII are broken down into more than 25 different genotypes (16, 18, 33). Genotypes in the GII genogroup are accountable for most of the human infection cases, while GI genotypes, known as Norwalk viruses, are commonly associated with shellfish ingestion outbreaks and waterborne transmission (18, 28). The genotype GII.4 has caused 70-80% of outbreaks and is associated with person-to-person transmission (28). GIII and GV genotypes contain bovine and murine noroviruses (MNVs), respectively (16).

Individual HuNoV strains are then named after the location in which they were first identified (16). For example, one HuNoV strain used in this study was the GII.4. Sydney (genogroup II, genotype 4) and first identified in Sydney, Australia in 2012 (35). Human norovirus GII.4 Sydney was the leading cause of acute gastroenteritis outbreaks in various countries, including the United States (35). Due to antigenetic drift, every two or three years a new strain will replace the once dominant strain (35).

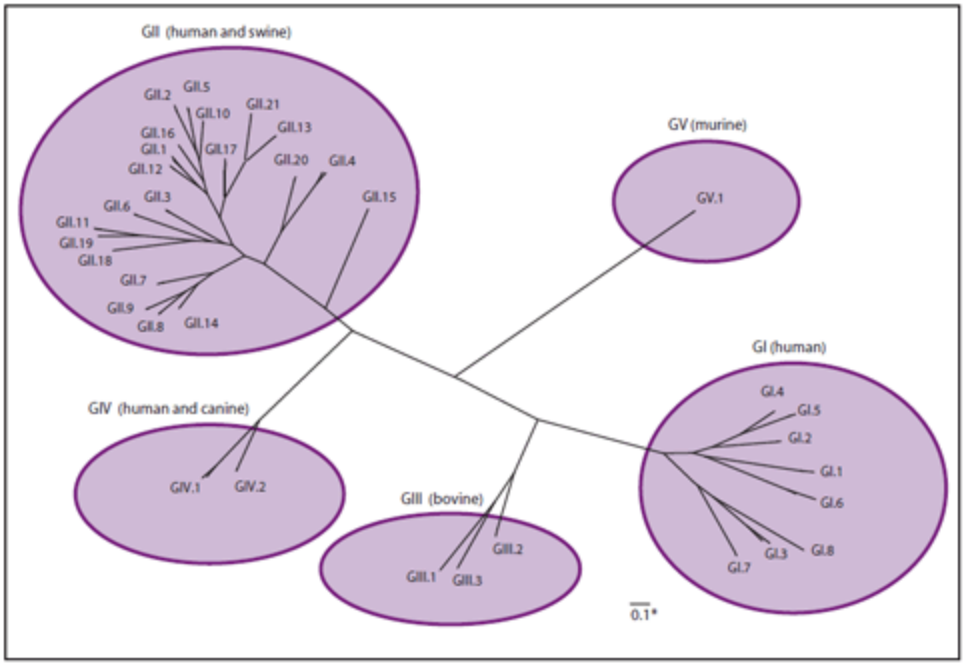

FIG 1 Classification of the *Norovirus* genus. * The scale bar represents the amount of amino acid substitutions at each site. (https://www.cdc.gov/mmwr/preview/mmwrhtml/rr6003a1.htm).

HuNoV Genome Organization

HuNoVs have a single-stranded, positive-sense RNA (+ssRNA) genome that is approximately 7.5 kb with three conserved open reading frames (ORFs) (Fig. 2) (18, 34). The 5’ end of the RNA is covalently attached to a viral protein genome-linked (VPg), which is a virus encoded protein, and the 3’ end is polyadenylated (31). Relatively short (approximately 50 nucleotides) untranslated regions (UTRs) appear on both ends of the genome. The UTRs contain conserved RNA secondary structures that are important for replication, translation, and pathogenesis (31). The first ORF encodes a nonstructural polyprotein that is cleaved by an encoded viral protease into six different proteins that are involved in viral replication (Fig. 2) (18, 31). The poly-protein includes: p48 (N-terminal protein), NTPase, p22, VPg, viral protease, and the viral RNA-dependent RNA polymerase (RDRP) (34). The second ORF encodes the VP1 protein that acts as the

major structural protein (Fig. 2). HuNoV capsids have 90 dimers of the VP1 protein and only one or two copies of VP2 proteins (31, 36). The VP1 capsid protein is 535-555 amino acids long and forms a T=3 icosahedral capsid. VP1 has two domains, the P (Protruding, P1 and P2 sub-domains) and S (shell) domains. The sub-domains of the P domain are essential for the capsid structure and stability. The P2 sub-domain is associated with the host cellular receptor binding sites and determination of viral serotypes. The receptor in hosts for HuNoVs hasn't been fully elucidated, but histo-blood group antigens (HBGAs) have been recognized as cofactors necessary for attachment (30, 34). HBGAs are complex carbohydrates that are attached to glycoproteins. In humans, HBGAs are found on red blood cells and mucosal epithelial cells, and bacteria such as *Enterobacter cloacae* have shown to express HBGAs as well. The S domain is essential for the icosahedral capsid formation (34)

ORF three encodes the VP2 protein that acts as the minor structural protein (Fig. 2) (18, 31). The VP2 capsid protein is 210-270 amino acids in length. In HuNoVs, VP2 exists in very low copy numbers and is a minor structural protein. Particles can assemble without VP2, but VP2 is necessary to make the particles infectious (34).

FIG 2 Genome organization of HuNoVs.

HuNoV Life Cycle

Due to a lack of convenient cell culture system, the complete life cycle of HuNoVs is not well documented. One discovery is that HuNoVs need to bind to HBGAs for attachment to host cells (15, 37). However, Jones *et al*. reported that HBGA

expression alone is not enough to allow infection of the GII.4. Sydney strain to cells in cell culture (38). Therefore, it is likely some unknown receptors/molecules are needed for the entry and infection of HuNoV (38, 39).

Once the norovirus genome is released into the cytoplasm, it becomes the template for translation since the norovirus genome is +ssRNA. The VPg that is covalently attached to the 5' end acts as a substitute for the 5' cap and aids in the translation of the viral RNA by binding translation initiation factors from the host. The VPg interacts with eIF4E and eIF3, along with the cap-binding protein to bring in the 43S ribosomal pre-initiation complex (31). eIF4A, which is the RNA helicase component of eIF4E is needed to unwind the secondary structures within the 5' end of the norovirus genome (31).

As with many other +ssRNA viruses, replication of the norovirus genome requires host intracellular membrane complexes (31). The membranes that house the replication complex come from the secretory pathway, including the trans-Golgi network, endosomes, and the endoplasmic reticulum (ER) (31). The p48 protein interferes with intracellular trafficking of host proteins and leads to Golgi degradation (36). The p48 mediated disassembly and rearrangement of the Golgi allows replication complexes for the viral RNA to assemble on intracellular membranes (36, 40). Along with the p48 protein, the p22 protein is also involved with Golgi disassembly and secretory pathway inhibition that also aids in the assembly of replication complexes (40).

Since noroviruses have a positive-sense genome, synthesis of a negative-sense RNA intermediate by the RDRP is done using the positive sense genome as a template. VPg is involved in genome replication by being a protein primer for RNA synthesis.

After the synthesis of the intermediate RNA strand, the new 5' positive-sense RNA strand and a subgenomic strand encoding VP1 and VP2 can be made, which will be used as the template for translation (31).

The mechanism for norovirus assembly and release is largely unknown. The VP1 proteins are able to self-assemble into virus-like particles (VLPs), which suggests this process aids in assembly during the life cycle (31). After virus assembly, the host cell is lysed, and the particles are released.

Progress in Cultivating HuNoVs

The difficulty in cultivating HuNoVs *in vitro* has been a main obstacle hindering related research. However, in the recent two years, some progress has been reported regarding cultivation of HuNoVs in cell culture (19, 38, 41).

In 2015, Jones *et al*. showed replication of the GII.4 Sydney strain in human B-cells (41). Human B-cells are a subset of lymphocytes that are derived from the bone marrow. A diverse array of antibodies are produced by B-cells that recognize and bind specific antigens (42). Jones *et al.* proposed that HuNoVs use enteric bacteria as a co-factor expressing HBGAs to infect B-cells (Fig. 3). It was shown that *E. cloacae* express HBGAs that GII.4. Sydney recognized. When unfiltered fecal samples of *E. cloacae* were added to the B-cell line, HuNoV GII.4. Sydney infectivity of B-cells was observed. When *Escherichia coli,* which did not express HBGAs was added, no rescue of infectivity occurred. The experiment showed HuNoVs binding with *E. cloacae* expressed HBGAs, causing HuNoV and bacteria to transcytose across the intestinal epithelial cells and allow HuNoV infection of B-cells (41).

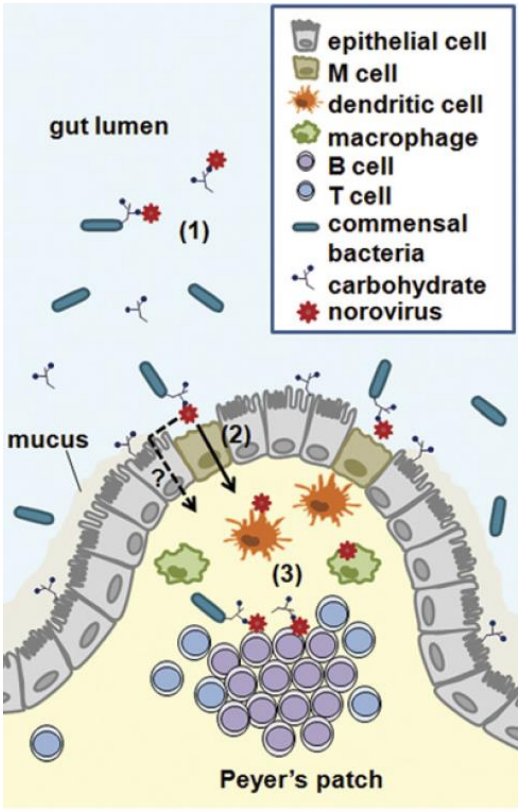

FIG 3 A model of how HuNoVs bind to HBGA as a co-factor expressed by enteric bacteria (1). The virus and bacteria transcytosed across the intestinal epithelial cells (2) and infect human B cells (3). (Photo courtesy of Karst and Wobus (43))

In 2015, Jones *et al.* developed a protocol based on their previous work detailing methods of cultivating GII.4 Sydney directly using human B-cells (38). In the protocol, unfiltered stool from an infected patient was used as inoculum. Unfortunately, there were limitations to the described protocol. First, the harvested virus from the B-cells was inconsistent, with a wide viral output range, which was 0.5 to 3.5-log fold increases in genome copy number (38). Second, the inoculum used for the virus cultivation was unfiltered fecal suspension. Although the unfiltered fecal material delivers enteric bacteria, a proposed cofactor for infection, unknown factors were also delivered within

the unfiltered material that influenced the susceptibility of B-cells to HuNoVs (38). The unknown factors within the unfiltered stool sample could be positively or negatively influencing the susceptibility of cultured B-cells. Results showed an inverse relationship with the input of virus levels and the efficiency of infection, possibly due to the unknown factors in the unfiltered stool (38). Lastly, and most importantly, the ability of obtaining successful HuNoV replication in other labs has been challenging (38). Different members from the CDC, University of Michigan, Erasmus Medical Center, University of Florida, and St. Jude Children's Research Hospital have had mixed results using this procedure to cultivate HuNoV (38).

The most recent attempt at cultivating HuNoVs used stem cell-derived human enteroids (intestinal cells) (19). Previous studies of cultivating HuNoVs in transformed intestinal epithelial cells and immune cells have not been completely successful (44, 45). Stem cells that were isolated from human intestinal tissue differentiated into the human intestinal enteroid cells (HIE), containing many epithelial cells such as enterocytes, goblet cells, enteroendocrine cells, and Paneth cells (19). To test the efficacy of the primary cell culture, a GII.4 norovirus was inoculated to the cell line and RT-qPCR identified a 1.5-2.5 log unit increase in the viral genome progeny at 96 hours post infection (19). The study suggested that bacteria were not required as cofactors due to the fecal suspension being filtered before inoculation. Even though the HIE cells contained multiple cell types, only the enterocytes were infected (19).

Given the HuNoV diversity, the research team wanted to know if other HuNoV strains could also replicate in HIEs. GI.1, GII.3, and GII.17 strains were used and no replication of these strains were observed (19). To try and observe replication, different

proteases, a requirement for other gastrointestinal virus replication, were added, but no replication occurred. Eventually the researchers pretreated the HIE cells with nontoxic levels of human bile and replication occurred in a dose-dependent manner for the GII.3 strain. It was observed that the addition of bile to GII.4 strains was not needed for replication to occur, but it increased the viral replication of the GII.4 strain. Therefore, these data suggested that there were certain strain-specific requirements to allow viral replication in the described system (19). Even though this is the best cell cultivation system to date, extensive research still needs to be done to determine what specific components are required for different HuNoV strains (19). There are still serious limitations to this procedure because the process is very new, complicated, and costly.

Surrogates for HuNoV

As mentioned, currently there is no convenient cell cultivation system available for HuNoVs (12, 13, 15). Therefore, one model for HuNoV research is using human volunteers. Volunteers have been used for medical, epidemiological, and inactivation studies of HuNoV (46, 47). Using human volunteers has given important information about the disease symptoms, persistence, and recovery (46, 47). Along with humans, gnotobiotic pigs have been successfully used as an animal model to study the pathogenesis of a HuNoV GII.4 strain (48). Lou *et al*. used gnotobiotic pigs to assess high pressure processing inactivation of a HuNoV GII.4 strain. (49). However, there are many limitations to using human volunteers and pig models. The research is expensive and requires strict regulations (46, 49). Therefore, most current inactivation studies on HuNoVs rely on cultivable surrogates, which include feline calicivirus (FCV), MNV, and Tulane virus (TV).

FCV belongs to the genus *Vesivirus* within the *Caliciviridae* family, and was the first calicivirus grown in cell culture and thus was the most widely used surrogate for HuNoVs (50). FCV has been used as a surrogate for the development of viricides and environmental stability studies (46). FCV has also been used as a model to study calicivirus translation and genome replication (46). However, FCV is not the best model for HuNoVs for two main reasons. First, FCV causes respiratory or systemic diseases but not gastrointestinal diseases (46). Second, discrepancies in the stability between HuNoVs and FCV were observed. Tung *et al.* showed continued HuNoV stability in 90% ethanol, whereas Malik *et al.* reported 99% inactivation of FCV in 70% ethanol (25, 51). Despite these major differences, the FCV has been crucial in the study of HuNoVs. Currently, FCV has been mostly replaced by other surrogates, such as MNV or TV.

MNV is also a common surrogate for HuNoVs and has largely replaced the FCV in HuNoV research (12, 14, 22, 52, 53). MNV was first propagated in cell culture in 2004 (50). This norovirus infects mice and belongs in genogroup V of the *Norovirus* genus (22). MNV is mostly cultivated in mouse macrophage cell lines (53, 54). MNV has been used in high-pressure, pH, temperature, and disinfection inactivation studies (12, 55–57). Another advantage for using the MNV as a surrogate is the ability of using mice as an animal model for experimental infections (53).

TV is in the *Recovirus* genus within the *Caliciviridae* family and was first cultivated in cell lines in 2008 (50, 58, 59). TV infects young rhesus macaques, one of the best known species of Old World monkeys, and are more closely related to humans than mice (59). The most common symptoms in rhesus macaques include gastroenteritis, respiratory infections, vesicular lesions, and hemorrhagic disease (59). Like HuNoVs, TV

is transmitted via the fecal-oral route and is shed in large numbers in stool. More importantly, TV recognizes HBGAs and can be grown in high titers in cell culture (58, 59). These properties make a convincing case for using TV as a cultivable surrogate virus for HuNoVs. In recent years, TV has been used as a surrogate in many different inactivation studies including high pressure, heat, UV, and ethanol treatments (12, 60, 61).

Even though studies using surrogates provide some useful information, the direct comparison of cultivable surrogates to HuNoVs could be inaccurate. A meta-analysis done by Knight *et al*. explains that HuNoVs are more persistent and resistant than cultivatable surrogates (62). HuNoVs and HuNoV surrogates can show different sensitivities to the same type of treatment and behave differently. Li and Chen demonstrated that a HuNoV GI.1 strain, a HuNoV GII.4 strain, MNV, and TV had different sensitivities to high hydrostatic pressure treatments and created a hierarchy of high hydrostatic pressure sensitivities of TV > GII.4 > MNV-1 > GI.1, from most to least sensitive (12).

Quantification of HuNoV

The ability to detect and accurately quantify infectious HuNoVs is extremely important, particularly for inactivation studies. In early studies, electron microscopy and antigen assays were used to quantify HuNoVs, which led to low quantification (13). Currently, detection and quantification of HuNoV mostly rely on molecular methods, particularly quantitative reverse transcription PCR (RT-qPCR). The use of RT-qPCR for detecting HuNoV has made a significant impact in the knowledge and understanding of norovirus epidemiology. However, quantifying HuNoVs directly by RT-qPCR is not able

to discriminate infectious from non-infectious particles because all viral RNA is being quantified, whether it was from an infectious or non-infectious virion. Applying RNase to degrade free viral RNA after treatment before RT-qPCR still overestimates the quantity of infectious viral particles because the genomic RNA can still be protected from RNase even if the capsid is damaged (15, 63). Scientists have tried different strategies to accurately quantify infectious HuNoVs (64, 65).

Aptamers

The use of aptamers is a new method for detection and quantification of HuNoVs. Aptamers are short single-stranded RNA or DNA segments that use tertiary nucleic acid structures that have binding affinity to a target (usually a protein) (66). Aptamers are selected and enriched via Systematic Evolution of Ligands by Exponential Enrichment (SELEX) (67). SELEX works by first synthesizing a large oligonucleotide library with random generated sequences typically 20-80 bases in length (67). The sequences are then exposed to the target. The sequences that do not bind the target by affinity chromatography are removed (68). The bound sequences are eluted and amplified by PCR. Eight to fifteen subsequent rounds of this selection take place with increasing elution stringency to find the sequences that bind the tightest to the target (67).

Once the target is recognized, the aptamers form secondary and tertiary structures. The tertiary structures allow the aptamers to bind to their targets via stable noncovalent bonds (Fig. 4) (68). The 3D structure of aptamers can now be used similarly to antibodies (63).

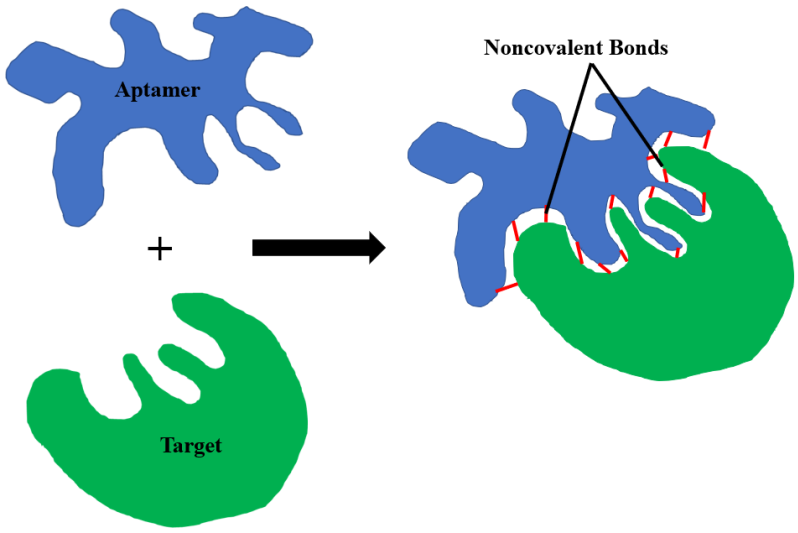

FIG 4 A simplistic diagram of an aptamer that recognizing a target sit and binding noncovalently to create an aptamer-target complex.

In the case of HuNoVs, nucleic acid aptamers have been selected based on their affinity towards the P domain of the VP1 capsid protein (66). Moore *et al*. attempted to produce ssDNA aptamers that were able to specifically bind the HuNoV. Through SELEX, the authors characterized two aptamers with high affinity for the P domain of the VP1 protein and the aptamers were able to bind serially diluted HuNoV GII.4 New Orleans in partially purified stool (66). Lastly, one of the developed aptamers was tested to estimate the ability of the aptamer to bind HuNoV VLPs after heat treatments (69). Moore *et al*. showed that the aptamer was able to quantify an 80% reduction of VLPs after treating VLPs at 75°C for one min (66, 69). However, the accuracy of using aptamers for HuNoV quantification is still unclear.

Propidium Monoazide (PMA)/RT-qPCR

PMA accompanied with RT-qPCR is another method for quantifying HuNoV (65). PMA is a photo-reactive nucleic acid dye that is able to bind the genome covalently (63, 65). For PMA to gain access to the nucleic acid, the cellular membrane or capsid of the target must be damaged. Once in the cell or virion, PMA intercalates into the nucleic acid and when exposed to high energy visible light, covalently binds to the nucleic acid (65). With the PMA intercalated, nucleic acid cannot be amplified by PCR. When a target is not compromised, PMA cannot access the nucleic acid. Without the intercalation of PMA into the genome, PCR can amplify the genome.

This method has be applied for the quantification of HuNoVs. Li *et al*. used PMA combined with RT-qPCR (PMA/PCR assay) to evaluate heat and high hydrostatic pressure treatments of HuNoVs (70). The PMA/PCR assay was able to quantify HuNoV reductions of up to 3 log units from heat and high hydrostatic pressure treatments (70). Karim *et al*. also applied this method to the inactivation of poliovirus, MNV, and HuNoV by heat, chlorine, and UV light (65). It was suggested that the PMA/PCR assay could differentiate infectious poliovirus from noninfectious poliovirus (65). However, the addition of PMA could not differentiate infectious and noninfectious when HuNoV was treated by heat, chlorine, and UV light (65). This study also suggests that viral capsid damage may be necessary for PMA to enter and bind to the viral genome as PMA/PCR assay was not able to differentiate between infectious and UV inactivated viruses (65).

PGM-MB/PCR Assay

Over the past few years, a pig (porcine) stomach (gastric) mucin (PGM) binding, conjugated with magnetic beads (MBs) followed by RT-qPCR (PGM-MB/PCR assay) has been applied to quantify infectious HuNoVs (12, 71, 72). Since PGM contains HBGAs, it can be used to bind to multiple strains of HuNoVs (12, 73). By linking PGM with MBs (PGM-MBs), particles with intact HBGA binding sites, bind to PGM-MBs, and can be separated from particles with damaged HBGA binding sites using a magnet (Fig. 5). The RNA from the bound virus particles can then be isolated and quantified by RT-qPCR (referred to here as PGM-MB/PCR assay) (12, 15). In addition, RNase can be added to degrade any RNA not protected by a capsid before PGM-MB binding (71).

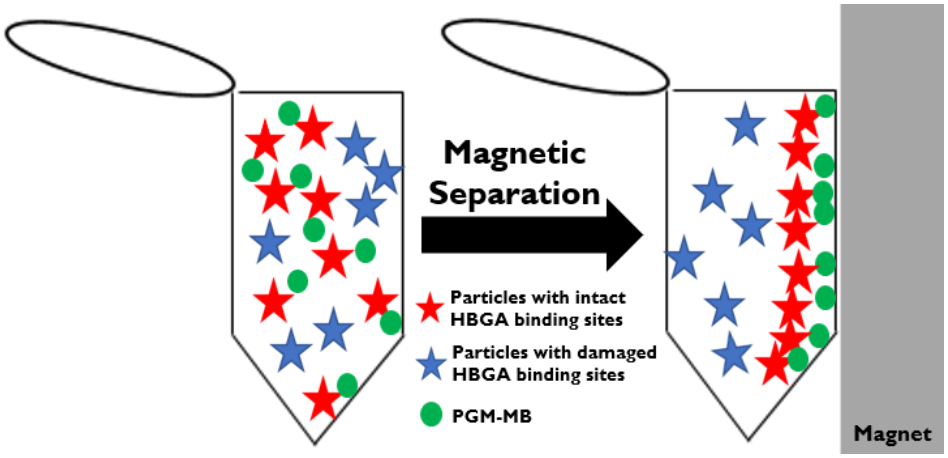

FIG 5 Simplified representation of PGM-MB binding to particles with intact HBGA binding sites

Based on the mechanism, this assay could be used to quantify infectious viral particles if the quantity of infectious viral particles correlates well with that of particles with intact HBGA binding sites. Therefore, in order to use this assay to accurately quantify infectious viral particles, it is important that the chosen inactivation procedures target capsid proteins or disrupt the viral capsid enough to inhibit binding to the PGM-

MBs as binding of PGM to the capsid is an essential step in this method (71). By using the PGM-MB/PCR assay, Tian *et al*. was able to capture and concentrate GI and GII HuNoVs in an oyster slurry and fruit/vegetable wash mixture, with a 2-log increase in detection sensitivity when compared to not using PGM-MB/PCR assay (73). By using this technique, Dancho *et al*. showed that untreated HuNoV GI.1 and GII.4 strains could bind to the PGM-MBs and achieve higher reductions compared RT-qPCR following only RNase treatment. Li and Chen also used this assay to assess the high hydrostatic pressure inactivation of MNV, TV, and HuNoV GI.1 and GII.4 strains. Results for MNV and TV assessed by PGM-MB/PCR were compared to those assessed by plaque assay (12). Li and Chen showed that the PGM-MB/PCR assay could quantify MNV and TV at <2-log reduction levels and would very likely be able to estimate high hydrostatic pressure inactivation of HuNoV. The PGM-MB/PCR assay was able to modestly quantify the inactivation of GI.1 strain at 2 to 3-log reduction and the GII.4 strain at 2 to 3.5-log reduction levels (12).

Antimicrobial Properties of Copper

The use of antimicrobial surfaces to inactivate infectious agents remain viable on surfaces can help reduce the risk of infections. Ever since the Egyptians began using copper for medical purposes between 2600 and 2200 BC, copper alloys have been recognized for their antimicrobial characteristics (13, 14). It has been documented that copper alloy surfaces can effectively inactivate bacteria, fungi, and viruses including methicillin-resistant *Staphylococcus aureus* (MRSA), and influenza H1N1 by degrading genetic material and disrupting the outer surface of the pathogen (13, 14). The use of copper was common until the use of antibiotics became available (74). The rise of

antibiotic resistant bacteria in hospitals, nursing homes, and other close quarter environments have increased the demand of alternative antimicrobial approaches (74). Copper alloy surfaces have also been used to decrease the spread of disease in hospitals when integrated into high-touch areas such as door knobs and bed rails. The results indicated a >50% reduction in an overall infection rate of healthcare-acquired infections (13, 75).

Copper is an essential trace element in most living organisms. There are more than 30 types of copper-containing proteins, including: cytochrome *c* oxidase, a terminal electron acceptor for the electron transport chain, and superoxide dismutase, an enzyme that mitigates oxidative damage (74). Even though copper is a necessary element, too much copper can be highly toxic. Through Fenton-like reactions, redox cycling between Cu (II) and Cu (I) can cause the creation of hydroxyl radicals that damage proteins and lipids (76). Copper ions can also compete for important protein binding sites with other essential metal ions, such as zinc and iron (74). Lastly, free copper ions are able to reduce sulfhydryl groups in proteins, which can lead to protein unfolding (74, 77).

Even though the exact mechanisms behind contact killing of bacteria due to copper is not exactly known, multiple aspects involved have been identified (78). One aspect is that copper ions dissolving from the copper surface causes direct cell damage by permeabilizing the cell membrane causing inner cellular solutes to spill out leading to cell death (76). Another aspect is that copper creates hydroxyl radicals that can cause further damage. Lastly, genomic and plasmid DNA can be degraded (78). It is not exactly known how DNA is damaged, but Warnes and Keevil suggest that damage is done directly by the copper ions and hydroxyl radicals, possibly by an influx of copper ions creating

unknown copper complexes with proteins that induce damage (78). Gram-negative bacteria such as *Escherichia coli*, *Salmonella enterica*, and other *Enterobacteriaceae* bacteria have been shown to be inactivated by copper (74). Copper has also been able to inactivate Gram-positive bacteria such as MRSA and *Listeria monocytogenes*, and it has been shown that certain spore-forming bacteria, like *Clostridium*, were killed after 24-48 hour treatment on copper surfaces (74, 79).

Copper has also been shown to inactivate enveloped viruses such as influenza, vaccinia virus, human corona viruses, and herpes simplex virus (80–82). The envelope of the viruses is damaged by the copper ions through generation of hydroxyl radicals and direct degradation. The destruction of the envelope allows copper ions and hydroxyl radicals to subsequently damage the viral genome (80). Studies from recent years also indicated that copper alloy surfaces could successfully inactivate non-enveloped viruses, such as HuNoVs and MNV by degrading the viral capsid and RNA genome (13, 14). Due to the lack of an envelope, copper damage might not occur through the generation of hydroxyl radicals (83). However, the efficacy of copper alloy surfaces for inactivation of HuNoVs has not been fully evaluated due to the difficulty of cultivating HuNoVs.

OBJECTIVES

This goal of this study was to determine the efficacy of copper alloy surfaces for the inactivation of TV using plaque assay and PGM-MB/PCR assay, and HuNoVs GII.4. Sydney and GI.3B. Potsdam using the PGM-MB/PCR assay. Based on the mechanism of the PGM-MB/PCR assay, it was likely this method could estimate the reduction more accurately if the inactivation method targets the capsid of TV and HuNoVs. Since copper treatments degrade the capsid of HuNoVs (13, 52), the PGM-MB assay would likely be able to evaluate the efficacies of copper alloy surface inactivation of HuNoVs (12). Results would provide useful information to determine if copper could serve as a potential precautionary measure to limit the spread of HuNoVs in close-quarter environments like schools, restaurants, and care facilities. The study included three main objectives:

1. **To compare the efficacy of different copper alloy surfaces for TV inactivation.**
2. **To compare PGM-MB/PCR and plaque assays for copper alloy surface inactivation of TV to determine the accuracy of PGM-MB/PCR assay.**
3. **To evaluate copper alloy surface inactivation of HuNoV GII.4. Sydney and GI.3B. Potsdam strains.**

MATERIALS AND METHODS

Viruses and Cell Line

Fecal suspensions of HuNoV GII.4. Sydney and GI.3B. Potsdam strains were generously provided by the Wisconsin State Laboratory of Hygiene. Fecal suspensions of the two HuNoV strains were centrifuged at 4,000 x *g* for 20 min. The supernatant was filtered through a 0.22 µm pore-size filter, aliquoted into convenient amounts, and stored at -80°C (12, 60). TV was generously provided by Dr. Xi Jiang at the Cincinnati Children's Hospital Medical Center. Rhesus monkey kidney epithelial cells LLC-MK2, purchased from ATCC were used to cultivate TV. M199 medium (Corning Cellgro, Manassas, VA) supplemented with 10% heat-inactivated fetal bovine serum (FBS, Gibco, Walthan, MA), and penicillin G (100 U/ml)-streptomycin (100 µg/ml, Gibco) was used to culture LLC-MK2 cells. TV was propagated in confluent monolayers of LLC-MK2. Crude unpurified TV stocks (referred to here as unpurified TV) were harvested from the cells via three freeze-thaw cycles followed by centrifugation to pellet the cell debris. The unpurified virus was stored at -80°C until use or further purified. The same published procedure for purification of murine norovirus was used to obtain purified TV stocks (14). Briefly, supernatant containing unpurified virus was purified using a 30% sucrose-cushion in an ultracentrifuge at 90,000 x *g* for 2.5 hours at 4°C. After centrifugation, the supernatant was removed, the pellet was resuspended in 3 ml phosphate-buffered saline (PBS, pH 7.2, Gibco). The sucrose cushion purified virus (referred to as purified TV here) was then aliquoted into convenient amounts and stored in -80°C until further use.

Metal Surface Preparation

Sheets of copper (100% Cu), bronze (90% Cu), brass (70% Cu), and stainless steel (0% Cu) were purchased online (http://www.onlinemetals.com/) and cut into ~2.5 × 2.5 cm coupons (Table 1). Before virus was placed on the coupons, surfaces were degreased in acetone, washed in distilled water and ultra-pure water, air dried, and sterilized.

TABLE 1 Composition of metal surfaces used in this study.

Metal (Unified Numbering System Designation)	% of Each Element				
	Cu	Zn	Ni	Fe	Cr
Copper (C11000)	100				
Bronze (C22000)	90	10			
Brass (C26000)	69-70	30-31			
Stainless Steel (T-304)			8	74	18

Surface Treatment of Viruses

Virus was treated on copper alloy surfaces following a published procedure with modifications (13). Purified and unpurified TV was used directly for inoculation, whereas GII.4. Sydney and GI.3B. Potsdam were both diluted three-fold in PBS (pH 7.2) before inoculation. For all experiments, 25 µl of virus was inoculated on each coupon and spread within a circle with a diameter of ~1 cm with the pipet tip. Depending on the metal used, virus was retrieved after either 2.5, 5, 10, 15, 20, or 40 min. Unpurified TV was retrieved from the coupon by pipetting up and down 25 times using M199 media, whereas purified TV and HuNoV strains were retrieved using PBS-EDTA [20 mM EDTA in PBS (pH 7.2)]. The amount of solution used to retrieve virus was determined based on the how much liquid containing the virus was left on the coupon at different treatment times and the final elute volume was ~100 µl. Eluted samples were then either directly diluted to be quantified by viral plaque assay or treated by 1µl of 10 mg/ml

RNase A (Thermo Schientific, Waltham, MA) at 37°C for 30 min after which virus was quantified by PGM-MB/PCR assay. Zero min treatments were used as controls for comparison with other treatment times. A negative control, liquid without virus, was included for treatments of each alloy for each replicate.

Viral Plaque Assay

Tulane virus was quantified by viral plaque assay that followed the procedures of Li and Chen (12). Briefly, confluent LLC-MK2 cells were first seeded in six-well plates. Cells were incubated for up to 24 hours until the monolayers were confluent. Cells were inoculated with 400 µl of ten-fold dilution series of TV. After inoculation, cells were incubated for one hour with gentle agitation every 10 mins at 37°C in a 5% CO_2 atmosphere. Cells were then overlaid with 2.5 ml of one-half volume M199 medium, 10% FBS, penicillin G (100 U/ml)-streptomycin (100 µg/ml)-amphotericin B (0.25 µg/ml, Gibco), and 0.5% agarose (Benchmark Scientific, Edison NJ). Plates were then incubated for four days at 37°C in a 5% CO_2 atmosphere. After incubation, cells were fixed with 3.7% formaldehyde (Fisher Scientific, Pittsburgh, PA) in PBS (pH 7.4, Corning Cellgro, Manassas, VA). Plaques were then counted by staining with 0.05% (w/v) crystal violet in 10% ethanol.

PGM-MB Preparation

PGM-MB preparation has been outlined in previous publications (12, 15). First, 1 ml of MagnaBind carboxyl-derivatized beads (Thermo Scientific) were washed with 1 ml PBS (pH 7.2) three times. A Bio-Rad SureBeads™ magnetic rack (Bio-Rad, Hercules, CA) was used to separate the beads perpendicular to gravity after each wash. One ml of 10 mg/ml type III mucin from porcine stomach (Sigma, St. Louis, MO) and 100 µl of 10

mg/ml 1-ethyl-3-[3-dimethylaminopropyl] carbodiimide hydrochloride (EDC, Thermo Scientific, Rockford, IL), both suspended in conjugation buffer (0.1 M MES [2-(*N*-morpholino) ethanesulfonic acid], 0.9% NaCl, pH 4.7, Thermo Scientific), were added to the magnetic beads and mixed on a Mini-Tube rotator (Fisher Scientific) at 4 rpm for 30 min. After mixing, beads were washed three times in 1 ml of PBS (pH 7.2) and then suspended in a 1 ml solution of 0.05% sodium azide in PBS (pH 7.2) and stored at 4°C.

PGM-MB Binding

The binding procedure was described previously with slight modifications (12, 15). After the RNase treatment of the copper alloy surface treated virus samples, 100 µl of PGM-MBs and 800 µl of PBS (pH 7.2, Gibco) were added to each sample. Samples were then placed on the rotator at 4 rpm for 15 min, allowing binding of the virus to the beads. After incubation, each sample was washed three times with 1 ml PBS (pH 7.2). Once the wash was complete, the samples were suspended in 140 µl of molecular biology grade water and put on ice until RNA extraction.

RNA Extraction

Viral RNA was extracted with the QIAamp viral RNA minikit (Qiagen, Valencia, CA) as described in previous publications (12, 15). Briefly, samples were lysed by Buffer AVL by QIAamp, and PGM-MBs were separated from the lysed supernatant by magnetic separation. The separated supernatant containing RNA was collected and used for the subsequent steps in the protocol. Lastly, RNA was eluted in 2x 40 µl AVE elution buffer and aliquoted for direct RT-qPCR quantification or stored at -80 °C.

RT-qPCR

The primers and TaqMan probe and their concentrations used in RT-qPCR for TV and both HuNoV strains were described previously with slight modifications (Table 2) (12, 84). All primers and probe were synthesized by Integrated DNA Technologies (Coralville, Iowa) or Thermo Fisher Scientific.

TABLE 2 List of primers and probes used in this study.

Primers/Probe	Sequence (5'→ 3')	Concentration (nM)	Reference
Tulane Virus			
p1888-F	TCGCGCAGCGCACTTA	900	(12)
p1889-R	CAAGAATCCAGAACAACCAATATCA	400	(12)
TVRdRp-P	FAM-CACCTTCTTGTGGGCCA-MGBNFQ	175	(12)
HuNoV GI.3B Potsdam			
QNIF4	CGCTGGATGCGNTTCCAT	500	(12, 84)
NV1LCR	CCTTAGACGCCATCATCATTTAC	900	(12, 84)
NVGG1p	(5'FAM/ZEN/3'IBFQ) TGGACAGGAGAYCGCRATCT	250	(12, 84)
HuNoV GII.4 Sydney			
QNIF2	ATGTTCAGRTGGATGAGRTTCTCWGA	500	(84)
COG2R	TCGACGCCATCTTCATTCACA	900	(84)
QNIFS	(5'FAM/ZEN/3'IBFQ) AGCACGTGGGAGGGCGATCG	250	(84)

All RT-qPCR reactions used the Fast Virus 1-Step Master Mix (Life Technologies, Carlsbad, CA). For each reaction, 10 µl reaction mixture consisted of 2.5 µl of Master Mix and 6 µl of template besides primers and probe. RT-qPCR assays were completed using a Bio-Rad CFX96 Touch™ Real-Time PCR Detection System (Bio-Rad). Conditions used for the RT-qPCR were 50°C for 5 min to allow reverse transcription, followed by 95°C for 20 s for initial denaturation, then 45 total cycles of 95°C for 3 s and 60°C for 1 min. Viral RNA extracted directly from virus stocks using QIAamp Viral RNA Mini kit was 10-fold serially diluted and used as standards. For each

RT-qPCR run, a set of standards were included to calculate the qPCR efficiency and log reductions achieved by the treatment. For GII.4. Sydney and GI.3B Potsdam, tenfold serial dilutions of viral samples made and prepared the same way but retrieved immediately from the coupons were included to determine the maximum log reductions of the two HuNoV strains. The detectable maximum reductions of GII.4. Sydney and GI.3B. Potsdam were 3 and 4 log units respectively. For data over the determined maximum log reductions, the maximum log reductions were used for calculations.

Statistical Analysis

At least three replicates were included for each experiment in this study. Log reductions were the differences between the 0 min treated samples and the treated samples at different times. One-sample *t*-test by comparing log reductions of treated samples to the fixed value 0 was performed to evaluate if significant reductions were achieved by treatments. Independent-samples t-test was performed to compare two groups and one-way ANOVA following Tukey's *post hoc* was performed to compare more than two groups. T-tests were not conducted for treatments with results of all replicates below detection limit and ANOVA post-hoc analysis results were not conducted for two treatments with results of all replicates below detection limit. Results were considered to be statistically significant with a p value <0.05.

RESULTS

Copper Alloy Surface Inactivation of Purified and Unpurified TV Assessed by Plaque Assay

In this study, unpurified TV was treated on copper and brass surfaces from 10 to 40 min and quantified by plaque assay. Results from plaque assay showed that 10 min copper and brass surface treatments of unpurified TV did not achieve any significant reduction (<1-log reduction) (Fig.6). However, copper surface treatments 15 min and longer of unpurified TV resulted in ~4-log reductions ($p<0.05$), and brass surface treatments 15 min and over of the same virus achieved ≤2-log reductions ($p<0.05$) (Fig. 6). Therefore, copper surface treatments 15 min and over of unpurified TV resulted in significantly higher reductions than brass surface treatments at the same treatment times ($p<0.05$) (Fig. 6).

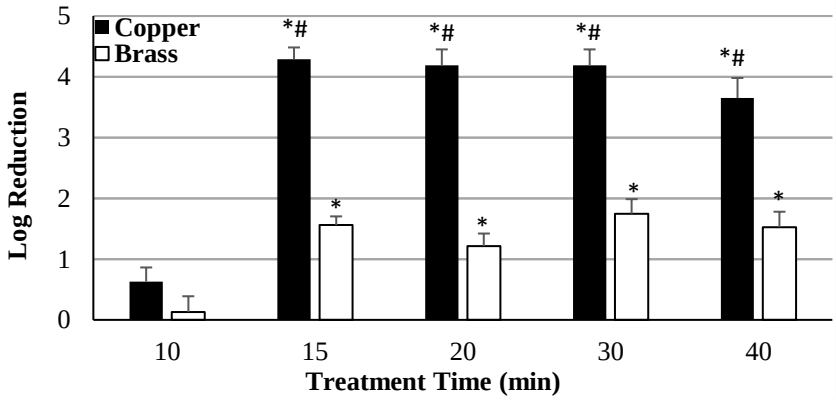

FIG 6 Copper and brass surface inactivation of unpurified TV assessed by plaque assay. Data are means of three replicates. Error bars represent one standard deviation. * denotes significant reductions ($p<0.05$) from one sample t-test by comparing log reductions of treated samples to the fixed value 0. # denotes that virus titers were below the detection limit (1.1-log units) in one or more of the replicates and the detection limit was used for log reduction calculations. The maximum detectable reduction for copper was 4.3±0.2 log units.

TV was then purified on a sucrose cushion, resuspended in PBS, and treated with copper, bronze, and brass surfaces for 2.5 to 20 min and quantified by plaque assay. Time-dependent inactivation of purified TV was observed with all copper alloys. All copper alloy surfaces were able to cause significant reduction of purified TV ($p<0.05$) at all treatment times (Fig. 7). One to 3-log reductions were observed when purified TV was treated for 2.5 or 5 min. As the treatment times of copper alloy surfaces reached 15 and 20 min, the titers of TV were reduced by at least 4.5 to 5 log units (Fig. 7). No significant difference in TV inactivation was observed among the different copper alloy surface treatments (Fig. 7). A stainless-steel surface was used for comparison and no more than 1-log reduction was achieved for treatment times of 10, 20, and 40 min (data not shown), indicating that the inactivation of TV was due to the copper alloy surfaces but not desiccation of the virus on the copper alloy surface.

Results from copper alloy surface inactivation of purified and unpurified TV also indicated that reductions of purified TV were significantly higher than those of unpurified TV during shorter exposures ($p<0.05$) (Fig. 6 and 7). For example, a 10 min copper surface treatment achieved around 4-log reduction of purified TV while <1-log reduction was achieved by the same treatment of unpurified TV ($p<0.05$) (Fig. 6 and 7). Ten, 15, and 20 min brass surface treatments of purified TV also resulted in significantly higher reductions (>3.5 log units) than achieved by the same treatments of unpurified TV (<2 log units, $p<0.05$) (Fig 6 and 7).

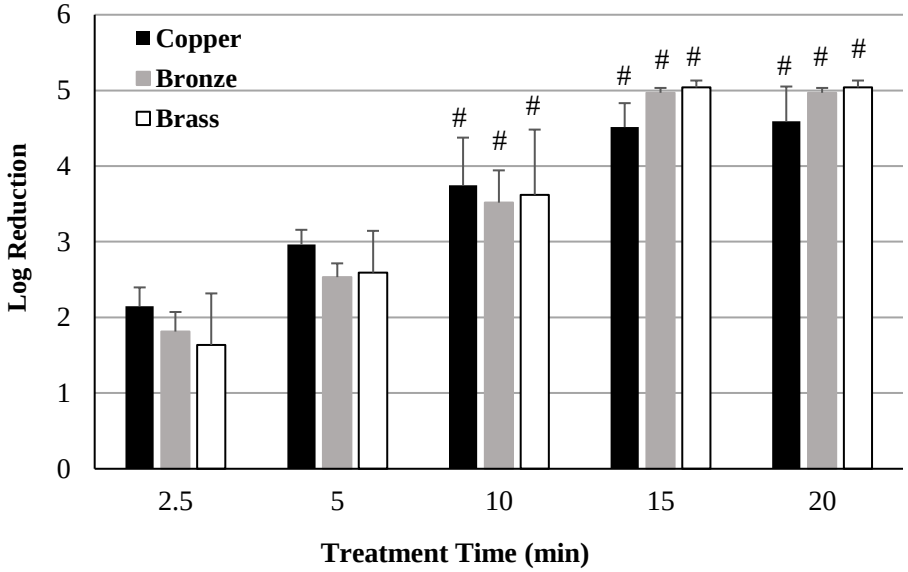

FIG 7 Inactivation of purified TV by copper, bronze, and brass surfaces assessed by plaque assay. Data are means of four replicates. Error bars represent one standard deviation. All metals at each treatment time achieved significant reduction of purified TV ($p<0.05$) analyzed by one sample t-test by comparing log reductions of treated samples to the fixed value 0. # denotes that virus titers were below the detection limit (1.1 log units) in one or more of the replicates and the detection limit was used for log reduction calculations. The maximum detectable reductions for copper, bronze and brass surface treatments of purified TV were 4.6±0.5, 5.0±0.1, and 5.0±0.1 log units, respectively. There was no significant difference among the log reductions by different copper alloys at the same treatment time.

Comparison of Results of PGM-MB/PCR and Plaque Assays

Besides plaque assays, copper and brass surface inactivation of purified and unpurified TV was also assessed via PGM-MB/PCR assay. Results from PGM-MB/PCR assay indicated that copper and brass surface treatments were also shown to demonstrate time-dependent reductions of purified TV (Fig. 8A). Even though 10, 15, and 20 min exposures of copper and brass surfaces all achieved significant reductions ($p<0.05$), the maximum reduction of purified TV by either copper or brass surfaces was 2.1 log units (Fig. 8A). In addition, although a brass treatment of purified TV for 2.5 min reached

significant reduction ($p<0.05$), it was only 0.2 log units (Fig. 8A). Additionally, the 20 min copper surface treatment of purified TV achieved a slightly higher reduction (2.1 log units) than a 20 min brass surface treatment (1.8 log units). No other significant difference between the log reductions of copper and brass surface treatments was observed ($p<0.05$) (Fig. 8A).

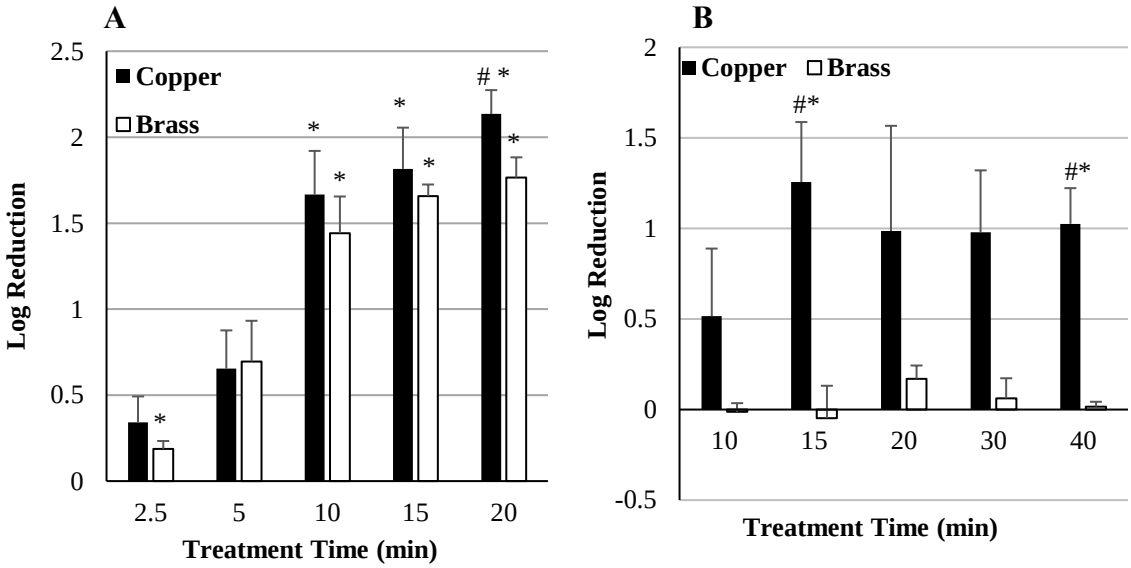

FIG 8 Copper and brass surface inactivation of purified TV (A) and unpurified TV (B) assessed by PGM-MB/PCR assay. Data are the means of 3 replicates. Error bars represent one standard deviation. * denotes significant reductions ($p<0.05$) from one sample t-test by comparing log reductions of treated samples to the fixed value 0. # denotes significant difference between copper and brass treatments at a particular treatment time ($p<0.05$).

When unpurified TV inactivation was assessed by the PGM-MB/PCR assay, no more than ~1.5-log reductions of unpurified TV were observed for any copper surface treatment times, and only 15 and 40 min copper surface treatments achieved significant, (but low) reductions (<1.5-log reductions, $p<0.05$) (Fig. 8B). Brass surface did not achieve any significant reduction (<0.5 log units) for any treatment of unpurified TV

(Fig.8B). Only 15 and 40 min copper surface treatments of unpurified TV achieved a significantly higher reductions than reductions from brass surface treatments for the same times ($p<0.05$) (Fig. 8B).

To determine the accuracy of the PGM-MB/PCR assay for the inactivation of TV, reductions of purified and unpurified TV assessed via PGM-MB/PCR assay were compared to those assessed via plaque assay. When compared to the results of PGM-MB/PCR assay, results for purified and unpurified TV from the plaque assay showed significantly higher reductions than those for the PGM-MB/PCR assay, when treated by both copper and brass surfaces at each treatment time ($p<0.05$) (Fig. 6, 7, and 8). For example, a 5 min copper treatment of purified TV achieved higher reduction (3 log units) as assessed via plaque assay than reduction from the same treatment assessed via PGM-MB/PCR assay (0.7 log units, $p<0.05$) (Fig. 7 and 8A). Similarly, 20 min copper and brass surface treatments of unpurified TV resulted in higher reduction (4.3 log units) assessed via plaque assay than reduction (1.3 log units) from the same surface treatment of unpurified TV assessed by PGM-MB/PCR assay (Fig. 6 and 8B). It should be noted that the maximum reductions of purified and unpurified TV assessed by PGM-MB/PCR assay were 2.1 log and 1.3 log units, respectively, whereas maximum reductions of purified TV and unpurified TV assessed by plaque assay were over 4 log unit for both purified and unpurified TV (Fig. 6, 7, and 8).

Copper Alloy Surface Inactivation of HuNoV GII.4 Sydney and GI.3B Potsdam

Besides TV, the PGM-MB/PCR assay was also used to assess copper alloy surface inactivation of HuNoVs. For GII.4 Sydney, a maximum detectable reduction of 3 log units for the PGM-MB/PCR assay was determined by using 10-fold serial dilutions of GII.4 Sydney for 0 min treatment following PGM-MB/PCR quantification. For any treatment achieving >3-log reduction of GII.4 Sydney, or no amplification of GII.4 Sydney RNA occurred, the RT-qPCR result was considered below the detection limit and 3 log units was used as the reduction for that treatment. Results showed that 2.5 and 5 min copper and brass surface treatments of GII.4 Sydney resulted in significant, but only ≤0.5-log reductions ($p<0.05$, Table. 3) while copper surface treatments of 10, 15 and 20 min and brass surface treatments of 15 and 20 min resulted in at least 3-log reductions of GII.4. Sydney (Table. 3) One-sample t-test and independent-samples t-test were not able to be conducted for the results of 10, 15 and 20 min copper surface treatments and 15 and 20 min brass surface treatments since the maximum detectable reduction (3 log units) was used for all replicates in those treatments. A stainless-steel surface treatment of GII.4 Sydney was also used for comparison and up to 40 min of stainless-steel surface treatment of GII.4 Sydney did not achieve more than 1-log reduction (data not shown).

TABLE 3 Copper alloy surface inactivation of HuNoV GII.4 Sydney and GI.3B Potsdam.

		Surface Treatment Time (min)				
HuNoV Strain	Surface	2.5	5	10	15	20
GII.4 Sydney	Copper	0.2±0.1*	0.5±0.0*	≥3.0±0.0#	≥3.0±0.0#	≥3.0±0.0#
	Brass	0.1±0.0*	0.3±0.1*	1.9±1.3#*	≥3.0±0.0#	≥3.0±0.0#
GI.3B Potsdam	Copper	ND	0.5±0.0*	≥4.0±0.0#	ND	≥4.0±0.0#

Data are the means of log reductions ± one standard deviation from three replicates. * denotes significant reductions ($p<0.05$) from one sample t-test by comparing log reductions of treated samples to the fixed value 0. # indicates results were below the detection limit for one or more of the replicates and the maximum detectable reductions were used for calculations. ND: Not Done.

Similar to the results for HuNoV GII.4 Sydney, results from copper treatments of GI.3B Potsdam showed that 5 min treatment resulted in a significant, but minimal 0.5-log reduction ($p<0.05$) (Table. 3). Following a similar procedure for determining the maximum detectable reduction for HuNoV GII.4 Sydney, the maximum detectable reduction for GI.3B Potsdam was determined to be 4 log units. Ten and 20 min copper surface treatments of GI.3B achieved at least 4-log reductions (Table. 3). Reduction of GI.3B from a stainless-steel surface treatment was similar to GII.4 (data not shown). No significant difference was observed between reductions of GII.4 Sydney and GI. Potsdam from a 5 min copper surface treatment. It was not possible to determine if there was significant difference between reductions of GII.4 Sydney and GI.3B Potsdam achieved by 10 and 20 min copper treatments, as the actual log reduction values are unknown.

DISCUSSION

HuNoVs are a significant public health concern, causing gastroenteritis around the world. These viruses show high stability in the environment and are able to remain infectious on surfaces for weeks (20). When trying to prevent or limit the spread of HuNoVs, it will be extremely useful if touch surfaces can inactivate HuNoVs. This study tested the efficacy of copper alloy surfaces for the inactivation of TV, a HuNoV surrogate, and HuNoVs.

As mentioned previously, HuNoVs cannot be conveniently cultivated in cell culture, therefore, surrogate viruses are often used. Various surrogates are used in inactivation studies, such as MNV, FCV, and TV (12, 14, 50, 60). This study used TV as a cultivable surrogate. TV is a suitable surrogate for several reasons. First, TV infects rhesus macaque monkeys, which are closely related to humans (32). Like HuNoVs, TV causes acute gastroenteritis that is cleared within days and has the same fecal-oral route of transmission. Lastly, TV can be cultivated in high titers and is able to also recognize HBGAs (12).

To our knowledge, TV has not been used as a surrogate to test for copper alloy surface inactivation. Results from this study indicated that copper alloy surfaces were able to effectively inactivate purified TV. For example, ~4-log reductions were observed when purified TV was treated with copper, bronze, and brass surfaces for at least 10 min. Inactivation of another HuNoV surrogate, MNV, by copper alloy surfaces has been investigated by other researchers (14). In that study, ~5-log reduction was observed when MNV was treated on a copper surface for 30 min (14). Copper alloy surfaces were also

very effective. Copper alloy surface treatments of 15 min and over were more effective in inactivating unpurified virus than brass treatments at the same treatment times. However, no difference was observed in reductions of purified TV caused by copper, bronze, and brass surface treatments.

Warnes *et al*. further determined how copper alloy surfaces inactivated MNV (14). By using transmission electron microscopy (TEM), Warnes *et al.* observed MNV to have irregular, uneven, and aggregative particles after copper alloy surface treatments, suggesting that the Cu(I) and Cu(II) ions were what gave copper the antimicrobial activity when degrading the viral capsid (14). The specific mechanism of damage to the capsid is unclear, but the copper ions either degrade the capsid by dissociating the capsomeres of the virus, or nonspecifically attacking the VP1 protein itself (14). Warnes and Keevil used non-denaturing agarose gel electrophoresis to show that the MNV RNA genome also gets degraded by copper alloy surfaces (83). By using different chelating reagents, Warnes and Keevil determined that even though Cu(II) ions are important for the antimicrobial activity, Cu(I) ions are the primary drivers of genome and capsid destruction by copper alloy surfaces (83).

Results from our study showed that copper alloy surfaces were more efficient at inactivating purified TV compared to unpurified TV. As assessed by plaque assay, when copper and brass surfaces treated unpurified TV, 10 min treatments of copper and brass surfaces achieved <1-log reductions while 10 min copper and brass surface treatments of purified TV achieved >4-log reductions. In our study, we did not investigate the reasons for the differences among the copper alloy surfaces for the inactivation of the two types of viral samples. However, it was likely that some substances in the unpurified TV

potentially hindered inactivation. The unpurified TV stock was the cell lysate, which included the M199 medium, containing inorganic salts, amino acids, vitamins, and FBS. In addition, it also included cellular proteins not pelleted during centrifugation. All the extra components in unpurified TV stock could have potentially interfered with the ability of copper ions to interact with the virus. Furthermore, pure copper, which contains more copper ions than a brass surface, would be more effective in inactivation of unpurified TV. When TV was purified by sucrose cushion and resuspended in PBS, most of the organic ingredients and other inorganic salts were removed. The lack of interference by the other components potentially allowed enough copper ions from each copper alloy surface to interact with purified TV so that no difference of inactivation efficacy among the different copper alloy surfaces of purified TV was observed.

Being able to accurately quantify HuNoVs is essential for studies about HuNoV inactivation. If cultivable surrogates are not used for HuNoV studies, molecular methods such as RT-qPCR are usually the alternative for quantification. When using only RT-qPCR, all RNA is being quantified, regardless if the virus is infectious or noninfectious, leading to overestimation of the quantity of infectious virus and underestimation of the inactivation efficacy.

In this study, the PGM-MB/PCR assay was used to quantify viral particles with intact HBGA binding sites, and therefore the degree of inactivation due to copper alloy surfaces. Li and Chen suggests that three assumptions are needed when using the PGM-MB/PCR assay, that if correct, would enable accurate quantification of infectious viral particles after a surface treatment: first, all the intact (infectious) virus particles not inactivated by the treatment must bind to PGM-MBs; second, all damaged

(noninfectious) virus particles inactivated by the treatment must not bind to PGM-MBs; third, from PGM-MB binding through RT-qPCR, there must not be any loss of bound virus particles throughout the whole assay (12). In addition, to have an accurate relationship between bound viral particles and infectious viral particles, it is important that treatment methods target the viral capsid instead of just the viral genome. This is because binding of the intact capsid of viral particles to PGM after treatment is an essential step in PGM-MB/PCR assay. If inactivation methods target the genome but leave the capsid intact, use of the PGM-MB/PCR assay would underestimate virus inactivation.

Since other studies suggested that copper damaged capsids of MNV and HuNoVs (13, 14, 83), it was reasonable to expect that copper would also target the capsid of TV and the PGM-MB/PCR assay should be able to estimate copper surface inactivation of TV (14). Therefore, in this study, we compared the results of copper alloy surface inactivation of TV assessed by PGM-MB/PCR assay with the results assessed by plaque assay to determine the accuracy of the PGM-MB/PCR assay.

Interestingly, results of copper alloy surface inactivation of purified TV assessed by PGM-MB/PCR assay did not match the results as assessed by plaque assay. Results from plaque assay showed higher reductions from copper alloy surface inactivation of purified and unpurified TV than those from PGM-MB/PCR. For example, results of PGM-MB/PCR assay showed that reductions no more than 2.1 log units were observed when purified TV was treated by a copper or brass surfaces for up to 20 min, whereas plaque assay results indicated greater than 4-log reductions achieved by 10, 15, and 20 min copper alloy surface treatments.

A similar phenomenon was also observed by Li and Chen when both plaque assay and PGM-MB/PCR assay were used to assess high hydrostatic pressure treatments of TV and MNV (12). In their study, both TV and MNV were treated by high hydrostatic pressure with different parameters, and PGM-MB/PCR assay showed no more than 2-log reductions achieved for both viruses while plaque assay showed maximum of ~3 and ~6-log reductions of TV and MNV, respectively. The reasons for the discrepancy between the reductions assessed by the plaque assay and PGM-MB/PCR assay in our study are still unclear (12).

Since higher reductions of copper alloy surface inactivation of TV were observed via plaque assay in our study, damaged TV that couldn't infect LLC-MK2 cells could seemingly still adequately bind to PGM and be quantified via RT-qPCR. It's possible that the capsid had some damage and was able to bind PGM, but unable to infect LLC-MK2 cells *in vitro*. To support this possibility, Aboubakr *et al*. observed that FCV particles were unable to infect host cells *in vitro*, but still retained their capsid structure when treated by cold atmospheric plasma for 15 sec (85). Similar to the speculation in Li and Chen's high hydrostatic pressure study, it was also possible that copper alloy surfaces damaged TV as a whole and the copper alloy surfaces were not preferentially damaging the specific HBGA binding sites on the TV capsid that bind to HBGA (12). In addition, other studies of copper surface inactivation of MNV and HuNoVs have shown that copper ions also degraded the viral genome (13, 83). Therefore, it is possible that during treatment, the RNA genome of some viral particles was damaged by copper ions to an extent without compromising the integrity of the capsids so that the viral particles were

unable to infect *in vitro,* but could still bind to PGM and be quantified by RT-qPCR, leading to overestimation of infectious virus.

Besides the studies of high hydrostatic pressure treatments of HuNoVs (12, 72), several other studies also used PGM-MB/PCR assay to evaluate the inactivation of HuNoVs by different treatments (70, 71, 73). Kingsley *et al.* used the PGM-MB/PCR assay to assess chlorine treatment of HuNoV (86). Using the PGM-MB/PCR assay, the researchers were able to observe significant reduction of HuNoV GI.1 and a HuNoV GII.4 strains after treatment of 100 ppm of chlorine (86). However, to our knowledge, the PGM-MB/PCR assay has not been used to assess copper alloy surface inactivation of HuNoVs.

In this study, HuNoV GII.4 Sydney and GI.3B Potsdam strains were used because of their epidemiological significance. Worldwide, it is reported that HuNoV GII.4 strains cause most norovirus infections (87). GII.4 Sydney accounted for over half of the outbreaks in the United States in 2012 and a new variant of GII.4 Sydney emerged and replaced the previous GII.4 Sydney strain as the dominant strain during the 2016-2017 season (87). GI HuNoVs are most often associated with outbreaks with food-borne and water-borne transmissions and a GI.3 HuNoV has caused an outbreak due to food contamination (28, 88).

In this study, we treated HuNoV GII.4 Sydney on copper and brass surfaces and GI.3B Potsdam on copper surface and assessed the inactivation via PGM-MB/PCR assay. Copper alloy surfaces were very effective surface treatments of both HuNoV strains. Ten minute copper surface treatments reduced both strains to below the detection limit, while 15 min brass surface treatments also reduced GII.4 Sydney to below the detection limit.

However, another study by Manuel *et al*. also evaluated copper alloy surface treatments of HuNoVs and showed that a 15 min copper alloy surface treatment reduced a GII.4 strain <1 log unit (13). There were differences between our study and the study by Manuel *et al*.(13).

Manual *et al*. used direct RT-qPCR with and without RNase for quantification (13). Because our study utilized the PGM-MB/PCR assay, the discrimination between infectious and noninfectious viral particles allowed a more accurate evaluation of copper surface efficacy (13). The method in which the virus was inoculated on the surface of the coupon could be another reason contributing to the difference of GII.4 reductions between the two studies (13). In our study, the inoculum was spread out within a circle with a diameter of ~1cm, allowing the inoculum to dry out in ~9-11 min. Maximum reductions were observed when the treatment times were long enough for the inocula to dry out compared to those at treatment times before the inocula dried out. Similarly, a study from Warnes *et al.* also suggests that if the inocula was able to quickly dry on a copper surface, MNV inactivation occurred more rapidly (83). Manuel *et al*. did not spread out the inoculum on the treatment surface, resulting in a drying time of ~20-30 min, which roughly correlated to the time it took the copper surface to reduce GII.4 ~3-log units (13).

Manuel *et al*. also reported that capsids of HuNoVs were damaged during exposure to copper alloy surfaces, which was consistent with another finding that copper alloy surfaces destroyed MNV capsids (13, 14). In the study by Manuel *et al.*, HuNoV GII.4 Grimsby VLPs were used for TEM, and GII.4 Houston VLPs were used for SDS-PAGE/Western blotting and HBGA binding analysis. The study found that copper

surface treatments caused aggregation and degradation of the VLPs after 60 min of treatment assessed by TEM (13). SDS-PAGE/Western blotting and HBGA binding analysis gave additional evidence of capsid degradation. After a 10 min exposure to a copper surface, the VP1 protein expression was ~25% of the VP1 protein from untreated VLPs, and lead to loss of nearly all ability to bind artificial HBGA (13). It has also been suggested that copper radical formation can attack histidine and proline amino acid residues (89). The P2 domain of VP1, the region thought to bind HBGA, has several histidine and proline amino acid residues (13, 90). Therefore, the decreasing number of viral particles of HuNoV bound to PGM-MB after copper alloy surface treatments, along with the results from Manuel *et al*., suggested that the inactivation by copper alloy surfaces could be occurring at the region where HuNoVs bind to HBGA (13). Further studies would be needed to evaluate this hypothesis.

This study demonstrated higher HuNoV reductions from copper alloy surface treatments than reductions observed with TV. This observation was not a total surprise, as Li and Chen observed a similar phenomenon when HuNoV strains, MNV, and TV were treated with high hydrostatic pressure and quantified by PGM-MB/PCR (12). Assessed by PGM-MB/PCR assay, Li and Chen observed a maximum of ~3.5 and 3-log reductions of a HuNoV GII.4 and a HuNoV GI.1 strains by high hydrostatic pressure, respectively, compared to the maximum 2-log reductions of MNV and TV treated by high hydrostatic pressure (12). Currently, more research is still needed to identify the potential reasons for the different reductions that could be achieved by HuNoVs and their surrogates.

Studies have indicated that different genogroups of HoNoVs could have different sensitivities to some treatments (12,72). Li and Chen observed that a HuNoV GI.1 strain was more resistant to high hydrostatic pressure than a HuNoV GII.4 strain using the PGM-MB/PCR assay (12). Lou *et al*. also used the PGM-MB/PCR assay to observe differences in sensitivities to high hydrostatic pressure among different genotypes within the same genogroup, and found different genotypes of the HuNoV GII genogroup showed different resistance to high hydrostatic pressure (GII.1>GII.6>GII.4) (72). To our knowledge, the difference of sensitivities of different genogroups of HuNoV to copper surface has not yet been examined. However, the results from our study could not indicate if sensitivities of GII.4 Sydney and GI.3B Potsdam to copper surface treatments were different or not because the actual reductions of both strains after copper surface treatments of 10 and 20 min were not known due to both strains achieving maximum detectable reductions. In the future, along with higher concentrations of HuNoV samples, if different copper alloys with different concentrations of copper, as well as different parameters are tested, results will provide additional information regarding the sensitivities of different HuNoVs to copper alloy surfaces.

In this study, we demonstrated that copper alloy surfaces can rapidly inactivate both TV, the HuNoV surrogate, and HuNoVs. Therefore, copper alloy surfaces can be used as an effective precautionary measure to limit the spread and infection of HuNoVs in close quarter environments like cruise ships, restaurants, and care facilities. Overall, even though PGM-MB/PCR assay underestimated the efficacy of copper alloy surface inactivation of TV, using this assay to quantify HuNoVs for some inactivation studies could still provide useful information. In addition, until a convenient method to cultivate

HuNoVs *in vitro* is developed, surrogates are still useful and have merits in certain inactivation studies.

REFERENCES

1. Todd EC, Grieg JD. 2015. Viruses of foodborne origin: a review. Virus Adapt Treat.7:25-45

2. Scallan E, Hoekstra RM, Angulo FJ, Tauxe RV, Widdowson M-A, Roy SL, Jones JL, Griffin PM. 2011. Foodborne illness acquired in the United States—major pathogens. Emerg Infect Dis 17:7–15.

3. Tung-Thompson G, Libera DA, Koch KL, Iii FL de los R, Jaykus L-A. 2015. Aerosolization of a human norovirus surrogate, bacteriophage MS2, during simulated vomiting. PLOS ONE 10:e0134277.

4. Thebault A, Teunis PFM, Le Pendu J, Le Guyader FS, Denis J-B. 2013. Infectivity of GI and GII noroviruses established from oyster related outbreaks. Epidemics 5:98–110.

5. Richards GP. 2012. Critical review of norovirus surrogates in food safety research: rationale for considering volunteer studies. Food Environ Virol 4:6–13.

6. Koopmans M, Duizer E. 2004. Foodborne viruses: an emerging problem. Int J Food Microbiol 90:23–41.

7. Koopmans M, von Bonsdorff C-H, Vinjé J, de Medici D, Monroe S. 2002. Foodborne viruses. FEMS Microbiol Rev 26:187–205.

8. Scallan E, Hoekstra RM, Angulo FJ, Tauxe RV, Widdowson M, Roy SL, et al. 2011. Foodborne illness acquired in the United States—major pathogens. Emerg Infect Dis 17:7-15.

9. Burnett E, Parashar U, Tate J. 2018. Rotavirus vaccines: effectiveness, safety, and future directions. Paediatr Drugs 1-11.

10. Aliabadi N, Tate JE, Haynes AK, Parashar UD. 2015. Sustained decrease in laboratory detection of rotavirus after implementation of routine vaccination — United States, 2000–2014. MMWR Morb Mortal Wkly Rep 64:337–342.

11. Cortese MM, Parashar UD. 2009. Prevention of rotavirus gastroenteritis among infants and children recommendations of the advisory committee on immunization practices. MMWR 58:1-25.

12. Li X, Chen H. 2015. Evaluation of the porcine gastric mucin binding assay for high-pressure-inactivation studies using murine norovirus and Tulane virus. Appl Environ Microbiol 81:515–521.

13. Manuel CS, Moore MD, Jaykus LA. 2015. Destruction of the capsid and genome of GII.4 human norovirus occurs during exposure to metal alloys containing copper. Appl Environ Microbiol 81:4940–4946.

14. Warnes SL, Summersgill EN, Keevil CW. 2015. Inactivation of murine norovirus on a range of copper alloy surfaces is accompanied by loss of capsid integrity. appl environ microbiol 81:1085–1091.

15. Li X, Chen H, Kingsley DH. 2013. The influence of temperature, pH, and water immersion on the high hydrostatic pressure inactivation of GI.1 and GII.4 human noroviruses. Int J Food Microbiol 167:138–143.

16. Karst SM. 2010. Pathogenesis of noroviruses, emerging RNA viruses. Viruses 2:748–781.

17. Patel MM, Widdowson M-A, Glass RI, Akazawa K, Vinjé J, Parashar UD. 2008. Systematic literature review of role of noroviruses in sporadic gastroenteritis. Emerg Infect Dis 14:1224–1231.

18. Atmar RL. 2010. Noroviruses - state of the art. Food Environ Virol 2:117–126.

19. Ettayebi K, Crawford SE, Murakami K, Broughman JR, Karandikar U, Tenge VR, Neill FH, Blutt SE, Zeng X-L, Qu L, Kou B, Opekun AR, Burrin D, Graham DY, Ramani S, Atmar RL, Estes MK. 2016. Replication of human noroviruses in stem cell-derived human enteroids. Science 353:1387–1393.

20. Hall AJ. 2012. Noroviruses: the perfect human pathogens? J Infect Dis 205:1622–1624.

21. Turcios RM, Widdowson M-A, Sulka AC, Mead PS, Glass RI. 2006. Reevaluation of epidemiological criteria for identifying outbreaks of acute gastroenteritis due to norovirus: United States, 1998–2000. Clin Infect Dis 42:964–969.

22. Hewitt J, Rivera-Aban M, Greening G e. 2009. Evaluation of murine norovirus as a surrogate for human norovirus and hepatitis A virus in heat inactivation studies. J Appl Microbiol 107:65–71.

23. Richards GP, Watson MA, Meade GK, Hovan GL, Kingsley DH. 2012. Resilience of norovirus GII.4 to freezing and thawing: implications for virus infectivity. Food Environ Virol 4:192–197.

24. Liu P, Yuen Y, Hsiao H-M, Jaykus L-A, Moe C. 2010. Effectiveness of liquid soap and hand sanitizer against norwalk virus on contaminated hands. Appl Environ Microbiol 76:394–399.

25. Tung G, Macinga D, Arbogast J, Jaykus L-A. 2013. Efficacy of commonly used disinfectants for inactivation of human noroviruses and their surrogates. J Food Prot 76:1210–1217.

26. Lopman B, Gastañaduy P, Park GW, Hall AJ, Parashar UD, Vinjé J. 2012. Environmental transmission of norovirus gastroenteritis. Curr Opin Virol 2:96–102.

27. Bartsch SM, Lopman BA, Ozawa S, Hall AJ, Lee BY. 2016. Global economic burden of norovirus gastroenteritis. PLoS ONE 11. e0151219

28. de Graaf M, van Beek J, Koopmans MPG. 2016. Human norovirus transmission and evolution in a changing world. Nat Rev Microbiol 14:421–433.

29. Bartsch SM, Lopman BA, Hall AJ, Parashar UD, Lee BY. 2012. The potential economic value of a human norovirus vaccine for the United States. Vaccine 30:7097–7104.

30. Cortes-Penfield NW, Ramani S, Estes MK, Atmar RL. 2017. Prospects and challenges in the development of a norovirus vaccine. Clin Ther 39:1537–1549.

31. Thorne LG, Goodfellow IG. 2014. Norovirus gene expression and replication. J Gen Virol 95:278–291.

32. Farkas T. 2015. Rhesus enteric calicivirus surrogate model for human norovirus gastroenteritis. J Gen Virol 96:1504–1514.

33. Lindesmith LC, Donaldson EF, Lobue AD, Cannon JL, Zheng D-P, Vinje J, Baric RS. 2008. Mechanisms of GII.4 norovirus persistence in human populations. PLoS Med 5:e31.

34. Zheng D-P, Ando T, Fankhauser RL, Beard RS, Glass RI, Monroe SS. 2006. Norovirus classification and proposed strain nomenclature. Virology 346:312–323.

35. He Y, Jin M, Chen K, Zhang H, Yang H, Zhuo F, Zhao D, Zeng H, Yao X, Zhang Z, Chen L, Zhou Y, Duan Z. 2016. Gastroenteritis outbreaks associated with the emergence of the new GII.4 Sydney norovirus variant during the epidemic of 2012/13 in Shenzhen City, China. PLOS ONE 11:e0165880.

36. Hardy ME. 2005. Norovirus protein structure and function. FEMS Microbiol Lett 253:1–8.

37. Huang P, Farkas T, Zhong W, Tan M, Thornton S, Morrow AL, Jiang X. 2005. Norovirus and histo-blood group antigens: demonstration of a wide spectrum of strain specificities and classification of two major binding groups among multiple binding patterns. J Virol 79:6714–6722.

38. Jones MK, Grau KR, Costantini V, Kolawole AO, de Graaf M, Freiden P, Graves CL, Koopmans M, Wallet SM, Tibbetts SA, Schultz-Cherry S, Wobus CE, Vinjé J, Karst SM. 2015. Human norovirus culture in B cells. Nat Protoc 10:1939–1947.

39. Almand EA, Moore MD, Jaykus L-A. 2017. Norovirus binding to ligands beyond histo-blood group antigens. Front Microbiol 8.

40. Roth AN, Karst SM. 2016. Norovirus mechanisms of immune antagonism. Curr Opin Virol 16:24–30.

41. Jones MK, Watanabe M, Zhu S, Graves CL, Keyes LR, Grau KR, Gonzalez-Hernandez MB, Iovine NM, Wobus CE, Vinjé J, Tibbetts SA, Wallet SM, Karst SM. 2014. Enteric bacteria promote human and mouse norovirus infection of B cells. Science 346:755–759.

42. LeBien TW, Tedder TF. 2008. B lymphocytes: how they develop and function. Blood 112:1570–1580.

43. Karst SM, Wobus CE. 2015. A working model of how noroviruses infect the intestine. PLOS Pathog 11:e1004626.

44. Lay MK, Atmar RL, Guix S, Bharadwaj U, He H, Neill FH, Sastry JK, Yao Q, Estes MK. 2010. Norwalk virus does not replicate in human macrophages or dendritic cells derived from the peripheral blood of susceptible humans. Virology 406:1–11.

45. Duizer E, Schwab KJ, Neill FH, Atmar RL, Koopmans MPG, Estes MK. 2004. Laboratory efforts to cultivate noroviruses. J Gen Virol 85:79–87.

46. Vashist S, Bailey D, Putics A, Goodfellow I. 2009. Model systems for the study of human norovirus biology. Future Virol 4:353–367.

47. Leon JS, Kingsley DH, Montes JS, Richards GP, Lyon GM, Abdulhafid GM, Seitz SR, Fernandez ML, Teunis PF, Flick GJ, Moe CL. 2011. Randomized, double-blinded clinical trial for human norovirus inactivation in oysters by high hydrostatic pressure processing. Appl Environ Microbiol 77:5476–5482.

48. Li J, Predmore A, Divers E, Lou F. 2012. New interventions against human norovirus: progress, opportunities, and challenges. Annu Rev Food Sci Technol 3:331–352.

49. Lou F, Ye M, Ma Y, Li X, DiCaprio E, Chen H, Krakowka S, Hughes J, Kingsley D, Li J. 2015. A gnotobiotic pig model for determining human norovirus inactivation by high-pressure processing. Appl Environ Microbiol 81:6679–6687.

50. Esseili MA, Saif LJ, Farkas T, Wang Q. 2015. Feline calicivirus, murine norovirus, porcine sapovirus, and Tulane virus survival on postharvest lettuce. Appl Environ Microbiol 81:5085–5092.

51. Malik YS, Maherchandani S, Goyal SM. 2006. Comparative efficacy of ethanol and isopropanol against feline calicivirus, a norovirus surrogate. Am J Infect Control 34:31–35.

52. Lou F, Neetoo H, Chen H, Li J. 2011. Inactivation of a human norovirus surrogate by high-pressure processing: effectiveness, mechanism, and potential application in the fresh produce industry. Appl Environ Microbiol 77:1862–1871.

53. Wobus CE, Thackray LB, Virgin HW. 2006. Murine norovirus: a model system to study norovirus biology and pathogenesis. J Virol 80:5104–5112.

54. Wobus CE, Karst SM, Thackray LB, Chang K-O, Sosnovtsev SV, Belliot G, Krug A, Mackenzie JM, Green KY, Virgin HW. 2004. Replication of norovirus in cell culture reveals a tropism for dendritic cells and macrophages. PLoS Biol 2. e432

55. Belliot G, Lavaux A, Souihel D, Agnello D, Pothier P. 2008. Use of murine norovirus as a surrogate to evaluate resistance of human norovirus to disinfectants. Appl Environ Microbiol 74:3315–3318.

56. Buckow R, Isbarn S, Knorr D, Heinz V, Lehmacher A. 2008. Predictive model for inactivation of feline calicivirus, a norovirus surrogate, by heat and high hydrostatic pressure. Appl Environ Microbiol 74:1030–1038.

57. Lee J, Zoh K, Ko G. 2008. Inactivation and UV disinfection of murine norovirus with TiO2 under various environmental conditions. Appl Environ Microbiol 74:2111–2117.

58. Drouaz N, Schaeffer J, Farkas T, Pendu JL, Guyader FSL. 2015. Tulane virus as a potential surrogate to mimic norovirus behavior in oysters. Appl Environ Microbiol 81:5249–5256.

59. Yu G, Zhang D, Guo F, Tan M, Jiang X, Jiang W. 2013. Cryo-EM structure of a novel calicivirus, Tulane virus. PLOS ONE 8:e59817.

60. Li X, Ye M, Neetoo H, Golovan S, Chen H. 2013. Pressure inactivation of Tulane virus, a candidate surrogate for human norovirus and its potential application in food industry. Int J Food Microbiol 162:37–42.

61. Tian P, Yang D, Quigley C, Chou M, Jiang X. 2013. Inactivation of the Tulane virus, a novel surrogate for the human norovirus. J Food Prot 76:712–718.

62. Knight A, Haines J, Stals A, Li D, Uyttendaele M, Knight A, Jaykus L-A. 2016. A systematic review of human norovirus survival reveals a greater persistence of human norovirus RT-qPCR signals compared to those of cultivable surrogate viruses. Int J Food Microbiol 216:40–49.

63. DiCaprio E. 2017. Recent advances in human norovirus detection and cultivation methods. Curr Opin Food Sci 14:93–97.

64. Xu S, Wang D, Yang D, Liu H, Tian P. 2015. Alternative methods to determine infectivity of Tulane virus: A surrogate for human nororvirus. Food Microbiol 48:22–27.

65. Karim MR, Fout GS, Johnson CH, White KM, Parshionikar SU. 2015. Propidium monoazide reverse transcriptase PCR and RT-qPCR for detecting infectious enterovirus and norovirus. J Virol Methods 219:51–61.

66. Moore MD, Escudero-Abarca BI, Suh SH, Jaykus L-A. 2015. Generation and characterization of nucleic acid aptamers targeting the capsid P domain of a human norovirus GII.4 strain. J Biotechnol 209:41–49.

67. Toh SY, Citartan M, Gopinath SCB, Tang T-H. 2015. Aptamers as a replacement for antibodies in enzyme-linked immunosorbent assay. Biosens Bioelectron 64:392–403.

68. Acquah C, Danquah MK, Yon JLS, Sidhu A, Ongkudon CM. 2015. A review on immobilised aptamers for high throughput biomolecular detection and screening. Anal Chim Acta 888:10–18.

69. Moore MD, Bobay BG, Mertens B, Jaykus L-A. 2016. Human norovirus aptamer exhibits high degree of target conformation-dependent binding similar to that of receptors and discriminates particle functionality. mSphere 1:e00298-16.

70. Li X, Huang R, Chen H. 2017. evaluation of assays to quantify infectious human norovirus for heat and high-pressure inactivation studies using Tulane virus. Food Environ Virol 1–12.

71. Dancho BA, Chen H, Kingsley DH. 2012. Discrimination between infectious and non-infectious human norovirus using porcine gastric mucin. Int J Food Microbiol 155:222–226.

72. Lou F, DiCaprio E, Li X, Dai X, Ma Y, Hughes J, Chen H, Kingsley DH, Li J. 2016. Variable high-pressure-processing sensitivities for genogroup II human noroviruses. Appl Environ Microbiol 82:6037–6045.

73. Tian P, Engelbrektson A, Mandrell R. 2008. two-log increase in sensitivity for detection of norovirus in complex samples by concentration with porcine gastric mucin conjugated to magnetic beads. Appl Environ Microbiol 74:4271–4276.

74. Grass G, Rensing C, Solioz M. 2011. Metallic copper as an antimicrobial surface. Appl Environ Microbiol 77:1541–1547.

75. Salgado CD, Sepkowitz KA, John JF, Cantey JR, Attaway HH, Freeman KD, Sharpe PA, Michels HT, Schmidt MG. 2013. Copper surfaces reduce the rate of healthcare-acquired infections in the intensive care unit. Infect Control Amp Hosp Epidemiol 34:479–486.

76. Borkow G, Gabbay J. 2005. Copper as a biocidal tool. Curr Med Chem Schiph 12:2163–75.

77. Santo CE, Lam EW, Elowsky CG, Quaranta D, Domaille DW, Chang CJ, Grass G. 2011. Bacterial killing by dry metallic copper surfaces. Appl Environ Microbiol 77:794–802.

78. Warnes SL, Keevil CW. 2011. Mechanism of copper surface toxicity in vancomycin-resistant enterococci following wet or dry surface contact. Appl Environ Microbiol 77:6049–6059.

79. Wheeldon LJ, Worthington T, Lambert PA, Hilton AC, Lowden CJ, Elliott TSJ. 2008. Antimicrobial efficacy of copper surfaces against spores and vegetative cells of *Clostridium difficile*: the germination theory. J Antimicrob Chemother 62:522–525.

80. Warnes SL, Little ZR, Keevil CW. 2015. Human coronavirus 229e remains infectious on common touch surface materials. mBio 6:e01697-15.

81. Bleichert P, Santo CE, Hanczaruk M, Meyer H, Grass G. 2014. Inactivation of bacterial and viral biothreat agents on metallic copper surfaces. BioMetals 27:1179–1189.

82. Sagripanti JL, Routson LB, Bonifacino AC, Lytle CD. 1997. Mechanism of copper-mediated inactivation of herpes simplex virus. Antimicrob Agents Chemother 41:812–817.

83. Warnes SL, Keevil CW. 2013. Inactivation of norovirus on dry copper alloy surfaces. PLOS ONE 8:e75017.

84. Stals A, Baert L, Botteldoorn N, Werbrouck H, Herman L, Uyttendaele M, Van Coillie E. 2009. Multiplex real-time RT-PCR for simultaneous detection of GI/GII noroviruses and murine norovirus 1. J Virol Methods 161:247–253.

85. Aboubakr HA, Mor SK, Higgins L, Armien A, Youssef MM, Bruggeman PJ, Goyal SM. 2018. Cold argon-oxygen plasma species oxidize and disintegrate capsid protein of feline calicivirus. PLoS ONE 13: e0194618

86. Kingsley DH, Fay JP, Calci K, Pouillot R, Woods J, Chen H, Niemira BA, Doren JMV. 2017. Evaluation of chlorine treatment levels for inactivation of human norovirus and MS2 bacteriophage during sewage treatment. Appl Environ Microbiol 83:e01270-17.

87. Yang Z, Vinjé J, Kulka M. 2017. Complete genome sequence of human norovirus GII.Pe-GII.4 Sydney from the United States. Genome Announc 5:e00159-17.

88. Nordgren J, Kindberg E, Lindgren P-E, Matussek A, Svensson L. 2010. Norovirus gastroenteritis outbreak with a secretor-independent susceptibility pattern, Sweden. Emerg Infect Dis 16:81–87.

89. Dean RT, Wolff SP, McElligott MA. 1989. Histidine and proline are important sites of free radical damage to proteins. Free Radic Res Commun 7:97–103.

90. Siebenga JJ, Vennema H, Renckens B, de Bruin E, van der Veer B, Siezen RJ, Koopmans M. 2007. Epochal evolution of GGII.4 norovirus capsid proteins from 1995 to 2006. J Virol 81:9932–9941.